AMERICAN SOCIETY FOR MICROBIOLOGY | mSystems®

RESEARCH ARTICLE

Identification of Effector Metabolites Using Exometabolite Profiling of Diverse Microalgae

Vanessa Brisson,[a] Xavier Mayali,[a] Benjamin Bowen,[b] Amber Golini,[b] Michael Thelen,[a] Rhona K. Stuart,[a] Trent R. Northen[b,c]

[a]Physical and Life Sciences Directorate, Lawrence Livermore National Laboratory, Livermore, California, USA
[b]Environmental Genomics and Systems Biology Division, Lawrence Berkeley National Laboratory, Berkeley, California, USA
[c]The DOE Joint Genome Institute, Lawrence Berkeley National Laboratory, Berkeley, California, USA

ABSTRACT Dissolved exometabolites mediate algal interactions in aquatic ecosystems, but microalgal exometabolomes remain understudied. We conducted an untargeted metabolomic analysis of nonpolar exometabolites exuded from four phylogenetically and ecologically diverse eukaryotic microalgal strains grown in the laboratory, freshwater *Chlamydomonas reinhardtii*, brackish *Desmodesmus* sp., marine *Phaeodactylum tricornutum*, and marine *Microchloropsis salina*, to identify released metabolites based on relative enrichment in the exometabolomes compared to cell pellet metabolomes. Exudates from the different taxa were distinct, but we did not observe clear phylogenetic patterns. We used feature-based molecular networking to explore the identities of these metabolites, revealing several distinct di- and tripeptides secreted by each of the algae, lumichrome, a compound that is known to be involved in plant growth and bacterial quorum sensing, and novel prostaglandin-like compounds. We further investigated the impacts of exogenous additions of eight compounds selected based on exometabolome enrichment on algal growth. Of these compounds, five (lumichrome, 5′-*S*-methyl-5′-thioadenosine, 17-phenyl trinor prostaglandin A2, dodecanedioic acid, and aleuritic acid) impacted growth in at least one of the algal cultures. Two of these compounds (dodecanedioic acid and aleuritic acid) produced contrasting results, increasing growth in some algae and decreasing growth in others. Together, our results reveal new groups of microalgal exometabolites, some of which could alter algal growth when provided exogenously, suggesting potential roles in allelopathy and algal interactions.

IMPORTANCE Microalgae are responsible for nearly half of primary production on earth and play an important role in global biogeochemical cycling as well as in a range of industrial applications. Algal exometabolites are important mediators of algal-algal and algal-bacterial interactions that ultimately affect algal growth and physiology. In this study, we characterize exometabolomes across marine and freshwater algae to gain insights into the diverse metabolites they release into their environments ("exudates"). We observe that while phylogeny can play a role in exometabolome content, environmental conditions or habitat origin (freshwater versus marine) are also important. We also find that several of these compounds can influence algal growth (as measured by chlorophyll production) when provided exogenously, highlighting the importance of characterization of these novel compounds and their role in microalgal ecophysiology.

KEYWORDS microalgae, exometabolome, effector metabolites, lumichrome, *Chlamydomonas reinhardtii*, *Desmodesmus*, *Phaeodactylum tricornutum*, *Microchloropsis salina*, *Chlamydononas reinhardtii*

Microalgae are important contributors to global carbon cycling, contributing almost 50% of photosynthetic carbon fixation (1). They are also important industrially for the production of biofuels and bioproducts (2, 3). The functionality and

Citation Brisson V, Mayali X, Bowen B, Golini A, Thelen M, Stuart RK, Northen TR. 2021. Identification of effector metabolites using exometabolite profiling of diverse microalgae. mSystems 6:e00835-21. https://doi.org/10.1128/mSystems.00835-21.

Editor Rosie Alegado, University of Hawaii at Manoa

Address correspondence to Vanessa Brisson, brisson2@llnl.gov.

Received 30 June 2021
Accepted 20 October 2021
Published 2 November 2021

stability of algal systems, both natural and engineered, are influenced by interactions of algae with other microorganisms and with each other, and exometabolites released into the water are important mediators of these interactions (4).

The specific compositions of algal exometabolite pools are important for modulating algal growth, and the interactions of algae and their associated communities through nutrient exchange, signaling, growth promotion and inhibition, and defense. A range of different plant hormones (indole-3-acetic acid, gibberellic acid, kinetin, 1-triacontanol, and abscisic acid) have all been shown to influence the growth of the model green alga *Chlamydomonas reinhardtii* (5). One strain of the coccolithophore *Emiliana huxleyi* has been shown to produce the plant hormone indole-3-acetic acid, while the growth of another strain was impacted by the same metabolite (6). Some algae have also been shown to inhibit the growth of competitor algae through the release of allelochemicals (7). Algal exudates have been hypothesized to play similar roles in the phycosphere, the microenvironment around algal cells, to those of root exudates in the rhizosphere (8). In plant systems, specific metabolites in root exudates have been shown to impact the growth of different microorganisms in the rhizosphere, favoring some microbial taxa over others (9). Similarly, combinations of metabolites known to be produced by algae have been shown to modulate microbial community composition depending on the combination of metabolites (10). In another study, rosmarinic acid and azelaic acid were shown to be produced by the diatom *Asterionellopsis glacialis* in response to bacterial presence and were also found to impact bacterial growth (11). Dimethylsulfoniopropionate produced by *E. huxleyi* feeds the bacterium *Phaeobacter inhibens*, but when the alga begins to produce *p*-coumarate, the bacterium responds by shifting its role from a mutualist, promoting algal growth, to a parasite, through the release of exometabolites (12).

Most studies of algal metabolomics have focused on the composition of intracellular metabolomes. For instance, of the organisms used in our study, the intracellular metabolomes of *Chlamydomonas reinhardtii* and *Phaeodactylum tricornutum* have been characterized for their responses to different growth conditions (13, 14). In contrast, microalgal exometabolomes, particularly for marine microalgae, have not been well characterized, partly due to the technical challenges of low metabolite concentrations and high salt content in the samples (15). Some recent studies have begun to analyze algal exometabolomes: Shibl et al. investigated the exometabolome of the diatom *Asterionellopsis glacialis*, and its response to the addition of a microbial community (11), while Ferrer-González et al. characterized the exometabolome of the diatom *Thalassiosira pseudonona* in comparison to cocultures of the diatom with three different bacterial strains (15). Another study used an untargeted metabolomics analysis to compare the exometabolomes of cyanobacteria (three *Prochlorococcus* strains and two *Synechococcus* strains) to diatoms (two *Thalassosira* species and one *Phaeodactylum*) (16). Metabolite exudation and uptake have also been studied in the cyanobacterium *Synechococcus* sp. strain PCC 7002 (17). To better understand microalgal interactions, there is a need to characterize exometabolites from a broader range of microalgae.

In this study, we characterized the nonpolar exometabolomes of four phylogenetically and ecologically diverse eukaryotic microalgal strains: the freshwater green alga *Chlamydomonas reinhardtii*, the brackish green alga *Desmodesmus* sp. strain C046, the marine diatom *Phaeodactylum tricornutum*, and the marine eustigmatophycean alga *Microchloropsis salina* (also referred to as *Nannochloropsis salina*). We chose these strains to cover a phylogenetically diverse group of microalgae with different environmental origins. *C. reinhardtii* and *Desmodesmus* are the most closely related of these algae, both belonging to the plant kingdom in the phylum Chlorophyta and the class Chlorophyceae. *P. tricornutum* and *M. salina* are both members of the kingdom Chromista but belong to different phyla. Additionally, *C. reinhardtii* and *P. tricornutum* are both model organisms that have been well studied and whose genomes have been sequenced (18, 19). *Desmodesmus* is also of particular interest because it can grow in both freshwater and saltwater, allowing us to examine metabolomic shifts under these two conditions. In addition to profiling the exometabolomes, the goal of

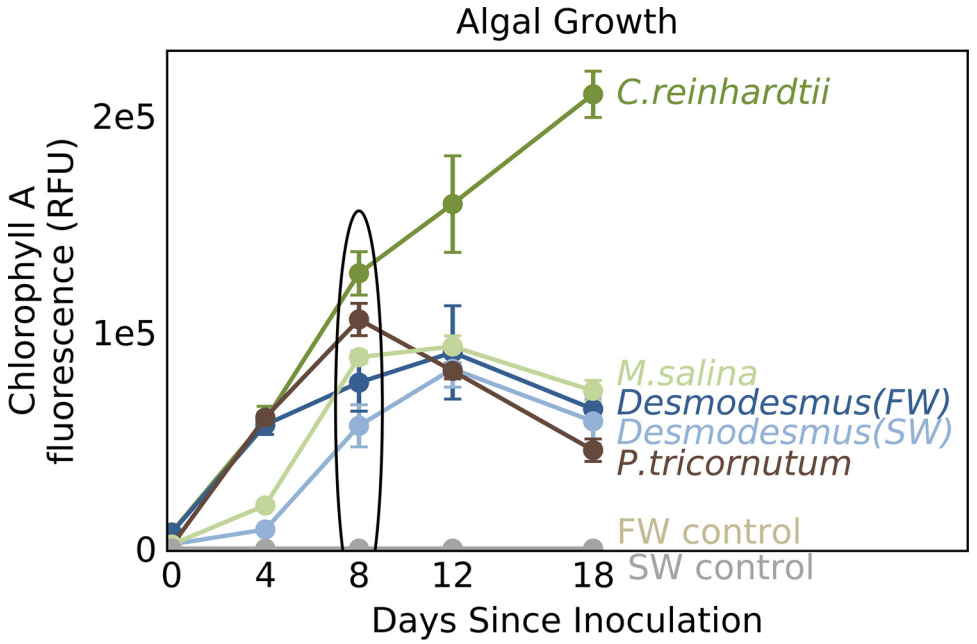

FIG 1 Algal growth as assessed by chlorophyll A fluorescence. Points and error bars indicate average fluorescence and standard deviation, respectively, of five biological replicates. The black oval indicates the day 8 samples, which were used for metabolite analysis. Chlorophyll A fluorescence is shown in relative fluorescence units (RFU).

our analysis was to determine whether specific exometabolites detected from these strains impacted algal growth and might therefore be effector metabolites involved in interactions within or between algal strains.

RESULTS

Algal growth. Algal chlorophyll fluorescence, an indicator of algal growth, increased with incubation time for all algal strains through the eighth day after inoculation, when samples were collected for metabolomic analysis (Fig. 1). Chlorophyll A fluorescence began to decrease by day 12 for *P. tricornutum* and by day 18 for all algal cultures except for *C. reinhardtii*, indicating that all cultures were in mid to late exponential growth when samples were collected. Ash-free dry weight measurements were made for the sampling times before and after day 8 (day 4 and day 12). Average biomass (ash-free dry weight) differed between the highest and lowest biomass alga by 1.6-fold on day 4 and 1.7-fold on day 12 (see Fig. S1a in the supplemental material). Increasing biomass between days 4 and 12 supports that at day 8 the algae were all in mid to late exponential growth.

The total organic carbon concentration of algal spent medium was measured for samples from day 8. Organic carbon concentrations ranged from 4 $\pm$ 2 ppm (330 $\pm$ 170 μM) for *Desmodesmus* (SW) to 13 $\pm$ 2 ppm (1,080 $\pm$ 170 μM) for *C. reinhardtii* (mean $\pm$ standard deviation for five replicates) (Fig. S1b). Based on these measurements, the total organic carbon loading from 30 ml spent medium onto solid-phase extraction columns ranged from 0.1 mg to 0.4 mg, well below the manufacturer listed maximum loading capacity of the columns (5 mg to 50 mg). Spent medium from algae grown in freshwater (*C. reinhardtii* and *Desmodesmus* [FW]) had higher concentrations of organic carbon than spent medium from algae grown in saltwater (*P. tricornutum*, *M. salina*, and *Desmodesmus* [SW]). Within each growth condition, the relative concentrations of organic carbon in spent medium followed the patterns of chlorophyll A fluorescence (*C. reinhardtii* > *Desmodesmus* [FW] and *P. tricornutum* > *M. salina* > *Desmodesmus* [SW]).

Metabolite profiles of diverse microalgae. To minimize matrix effects resulting from differences in salt concentrations, we focused on nonpolar metabolite analysis using both C_{18}-based solid-phase extraction and C_{18}-based liquid chromatography. It is important to note that this extraction method recovers only a fraction of the dissolved organic carbon

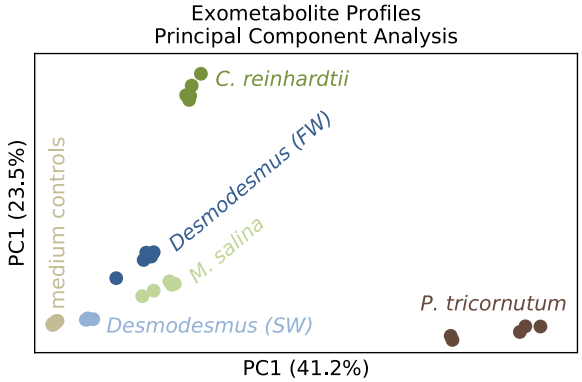

FIG 2 Principal-component analyses of algal exometabolite profiles. Each point represents one of five replicate samples per alga or control condition. Colors indicate which algal culture the sample was from as follows: gray, medium controls; brown, *P. tricornutum*; light green, *M. salina*; dark green, *C. reinhardtii*; light blue, *Desmodesmus* (FW); dark blue, *Desmodesmus* (SW).

present in the sample and is biased toward recovery of nonpolar metabolites. To assess matrix effects on metabolite detection, we analyzed detection of ^{13}C- and ^{15}N-labeled internal standards. Signal suppression of internal standards was generally low and comparable across sample groups, with the exception of the saltwater exometabolite samples (Fig. S2). For saltwater exometabolite samples, the median $\log_2$ fold change compared to the value for extraction controls ranged from -1.4 to -2.0 for the different sample groups. For all other sample groups, median $\log_2$ fold change ranged from -0.15 to -0.68.

Initial untargeted analysis of liquid chromatography-tandem mass spectrometry (LC-MS/MS) data for all cell pellet, spent medium, and control samples detected 14,916 features, of which 4,259 features were determined to be significantly different from medium blank controls (adjusted *P* value of <0.05 and fold change compared to control value of >2) for at least one sample group, where a sample group consisted of all five replicates for a single organism and sample type (cell pellet or spent medium) combination (see Data Set S1 in the supplemental material).

Within the subset of significant features, overall exometabolome composition differed between the different algal cultures (Fig. 2). Principal-component analyses of the exometabolite profiles separated samples from the different algae, including separating metabolite profiles for *Desmodesmus* grown in freshwater from *Desmodesmus* grown in saltwater (Fig. 2). The first two principal components accounted for a total of 67.4% of the variance in exometabolite profiles. Saltwater cultures separated along the first principal-component axis, and freshwater cultures separated largely along the second principal-component axis.

Hierarchical clustering of LC-MS/MS (Fig. 3, top dendrogram) revealed distinct sets of predominantly cell pellet features (gray) and predominantly extracellular features (purple), as well as distinct sets of features associated with the different algal strains. Across all 4,259 features and sample groups (sample type and organism), the median $\log_2$ fold change in one sample group compared to the sample group with maximum signal was -5.6, corresponding to a 48.4-fold change. Hierarchical clustering of samples (Fig. 3, side dendrograms) indicated that *Desmodesmus* metabolite profiles from freshwater and saltwater were distinct but were more similar to each other than to metabolite profiles from other algae. Further, although *Desmodesmus* and *C. reinhardtii* are more closely related to each other than to the other algae, their metabolite profiles did not cluster together in the hierarchical clustering analysis. To further assess whether the metabolite profiles correlated with phylogeny, we conducted a Mantel test comparing phylogenetic distances between algae to Euclidean distances between normalized exometabolite profiles. That test did not detect any significant correlation between phylogeny and exometabolome ($r = 0.07$ and P value $= 0.29$ when the saltwater metabolite profiles were used for

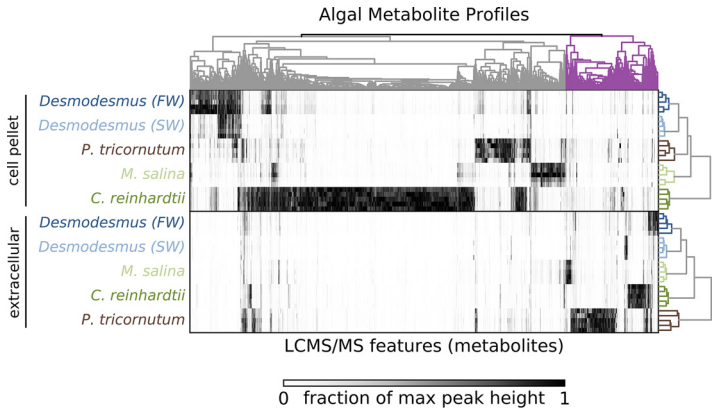

FIG 3 Heatmap of algal metabolite signal intensities. Samples (five replicates per alga) are represented in rows, and metabolites are represented in columns. Shading at each point indicates the level of a feature in a particular sample as measured by the fraction of the maximum signal intensity for that feature. The top dendrogram shows hierarchical clustering of metabolites. The side dendrograms show hierarchical clustering of samples for extracellular and cell pellet samples.

Desmodesmus and $r = 0.17$ and P value = 0.17 when the freshwater metabolite profiles were used).

To obtain putative annotations for some features and to assess potential relationships between features through feature-based molecular networking, we analyzed the peak detection results with the Global Natural Products Social Molecular Networking (GNPS) tool (20, 21). This analysis resulted in preliminary spectral matches for 263 features based on tandem mass spectrometry (MS2) mass spectra, of which 137 (52%) had signal intensities at least twofold greater than controls for at least one sample group (see Table S1 in the supplemental material). This represents 3.2% of all 4,259 features that were significantly greater than medium controls. For features of interest discussed below, we manually curated the best spectral matches (from up to 100 matches per feature) based on the GNPS cosine score, delta *m/z*, number of shared peaks, and adducts. Final curated annotations are listed in Table S1. Only the features with the highest quality matches (GNPS cosine score of >0.7, delta *m/z* of <10 ppm, number of shared peaks > 5, common adducts: $[M+H]^+$ or $[M+Na]^+$ for positive mode or $[M-H]^-$ or $[M+Cl]^-$ for negative mode) were considered putative annotations due to a lack of retention time information for authentic standards, with a metabolomics standards initiative (MSI) level 2 identification (22, 23). Two metabolites were subsequently confirmed using authentic standards as described below.

Characterization of algal exudates. To differentiate metabolites resulting from lysis versus exudation, we identified features significantly enriched in the exometabolome in paired samples of extracellular and cell pellet metabolites. Enrichment was assessed based on the ratio of peak heights between paired exometabolome and cell pellet samples. Because of inherent differences between sample types, this ratio should be interpreted as a qualitative estimate of enrichment. Of the 138 features with spectral matches from GNPS, 41 (29%) were significantly enriched in the exometabolome of at least one alga (Fig. 4). Enrichment ratios for these features ranged from 2.1 to infinite (feature not detected in cell pellet), with a median enrichment ratio of 6.3.

Although most exometabolome-enriched features were enriched in the spent medium of only one alga, two features (positive features 4889 and 7957, identified as lumichrome and 5′-*S*-methyl-5′-thioadenosine, respectively) were enriched in four of the five algal systems tested. The identities of these features were further confirmed by matching retention times to standards analyzed in our laboratory, resulting in MSI level 1+ identifications. The levels of lumichrome and 5′-*S*-methyl-5′-thioadenosine differed between algal cultures, with *P. tricornutum* producing the highest levels of both metabolites among the exometabolomes (Fig. S3). Additionally, four features were

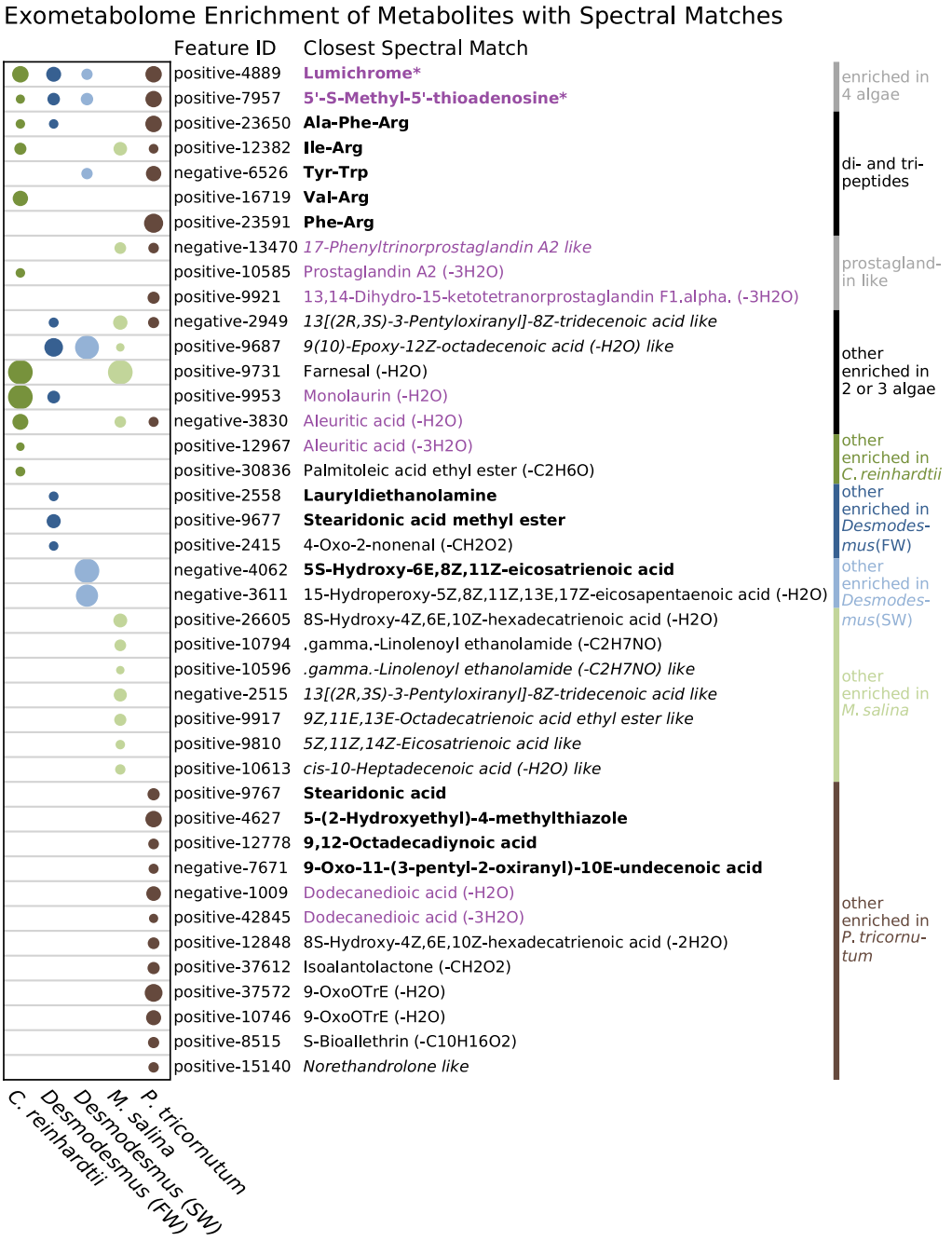

FIG 4 Exometabolome-enriched metabolites with putative annotations. Circle sizes are proportional to the base 2 logarithm of the average relative enrichment ratio in the exometabolome compared to the cell-associated metabolome for five biological replicates. MSI level 1+ identified compounds are indicated with an asterisk. Spectral matches in bold type indicate high-quality putative annotations (MSI level 2). Spectral matches in plain (roman) type indicate quality matches to unusual adducts, suggesting related molecules with different chemical formulae, with potential difference indicated in parentheses (MSI level 3). Spectral matches in italic type indicate matches with high *m/z* error, suggesting different, but potentially related compounds. Spectral match names in purple were selected for exogenous metabolite addition experiments.

enriched in three of the algal systems, and three were enriched in two of the algal systems (Fig. 4).

Three features potentially related to prostaglandins were enriched in the exometabolomes of some algae, with at least one of these features enriched for all algal strains tested except *Desmodesmus*. Across the full data set, seven features had best spectral matches to

prostaglandins, all with either spectral matches to unusual adducts or had *m/z* errors greater than 10 ppm, indicating that these were not exact matches but instead represented potentially related compounds. To further understand this group of features, we evaluated these features in the context of the GNPS feature-based molecular networking analysis (20), which resulted in five subnetworks containing features with spectral matches to prostaglandins (Fig. S4). The features in these subnetworks were generally associated with individual algal strains, with different features being dominated by different strains. In addition to prostaglandin-like features, others had high spectral similarity to steroids and other lipids. Moreover, many of the edges in the molecular network (linking two features with similar spectra) corresponded to *m/z* differences indicating the specific loss or gain of small numbers of carbons and hydrogens (C_2H_2, C_4H_4, etc.), suggesting that this may represent a related group of lipids with small variations in chemical formulae.

Several features putatively annotated (MSI level 2) as dipeptides and tripeptides were also enriched in the exometabolomes of the different algae, with each alga having at least one of these enriched in its exometabolome. These features (positive features 23650, 12382, 12591, and 16719 and negative feature 6526) were putatively annotated as Ala-Phe-Arg, Ile-Arg, Phe-Arg, Val-Arg, and Tyr-Trp, respectively. Across the full data set, di- and tripeptide features were highly associated with the exometabolomes compared to cell pellet metabolomes, with the exception of Arg-Trp which was most abundant in the cell pellet metabolome of *C. reinhardtii* (Fig. S5).

Impact of exudate metabolites on algal growth. Based on the enrichment of specific features in the exometabolomes of one or more algal cultures, eight metabolites were selected to evaluate their impacts on algal physiology and growth. The selected metabolites were 13,14-dihydro-15-keto-prostaglandin F1-α, 17-phenyl trinor prostaglandin A2, prostaglandin A2, 5′-*S*-methyl-5′-thioadenosine, lumichrome, monolaurin, aleuritic acid, and dodecanedioic acid (exometabolome enrichment of features is shown in Fig. 4). Five of the added metabolites had significant and distinct effects on growth for each of the algal strains when added at a concentration of 0.01 mM (Fig. 5). Most significant was dodecanedioic acid, which impacted growth in all cultures, decreasing growth of *C. reinhardtii*, *Desmodesmus* (FW), and *P. tricornutum* (65%, 14%, and 23%, respectively) and increasing growth of *Desmodesmus* (SW) and *M. salina* (44% and 48%, respectively) (Fig. 5). Aleuritic acid had opposite effects on the two freshwater cultures, increasing *C. reinhardtii* growth and decreasing *Desmodesmus* freshwater growth (Fig. 5). Lumichrome, 5′-*S*-methyl-5′-thioadenosine, and 17-phenyl trinor prostaglandin A2 increased growth in *P. tricornutum* (17%, 19%, and 20%, respectively), and the last two decreased growth in *Desmodesmus* in freshwater. Impacts of some metabolites were concentration dependent (e.g., impacts of dodecanedioic acid on all algae except *Desmodesmus* [FW]), while others (e.g., increase in *P. tricornutum* growth with lumichrome, 5′-*S*-methyl-5′-thioadenosine, and 17-phenyl trinor prostaglandin A2) maintained similar effects at all concentrations tested (0.01, 0.001, and 0.0001 mM) (Fig. S6).

Response of *Desmodesmus* to medium conditions. *Desmodesmus* sp. strain C406 is unique among the algae tested here in its ability to grow in both the saltwater and freshwater medium. Between the two growth media, both the extracellular and cell pellet metabolite profiles differed significantly. Because high salt concentrations can interfere with detection of compounds by LC-MS/MS, making some metabolites appear to be lower or not detectable from high salt samples due to matrix effects (24, 25), we focused on metabolites that were detected at significantly higher levels in the saltwater samples. Three features with spectral matches to database compounds were significantly enriched in the exometabolome of *Desmodesmus* grown in saltwater compared freshwater (Fig. S7). These enriched features included the putatively annotated dipeptides Tyr-Trp and Arg-Trp, as well as negative feature 1013, which had high spectral similarity to the $[M\text{-}H\text{-}H_2O]^-$ adduct of dodecanedioic acid. Several of the metabolites resulted in decreased growth in *Desmodesmus* (FW) but did not have significant effects on *Desmodesmus* (SW). Notably, in the exogenous metabolite addition experiment above, *Desmodesmus* responded positively (44% increase in chlorophyll A) to

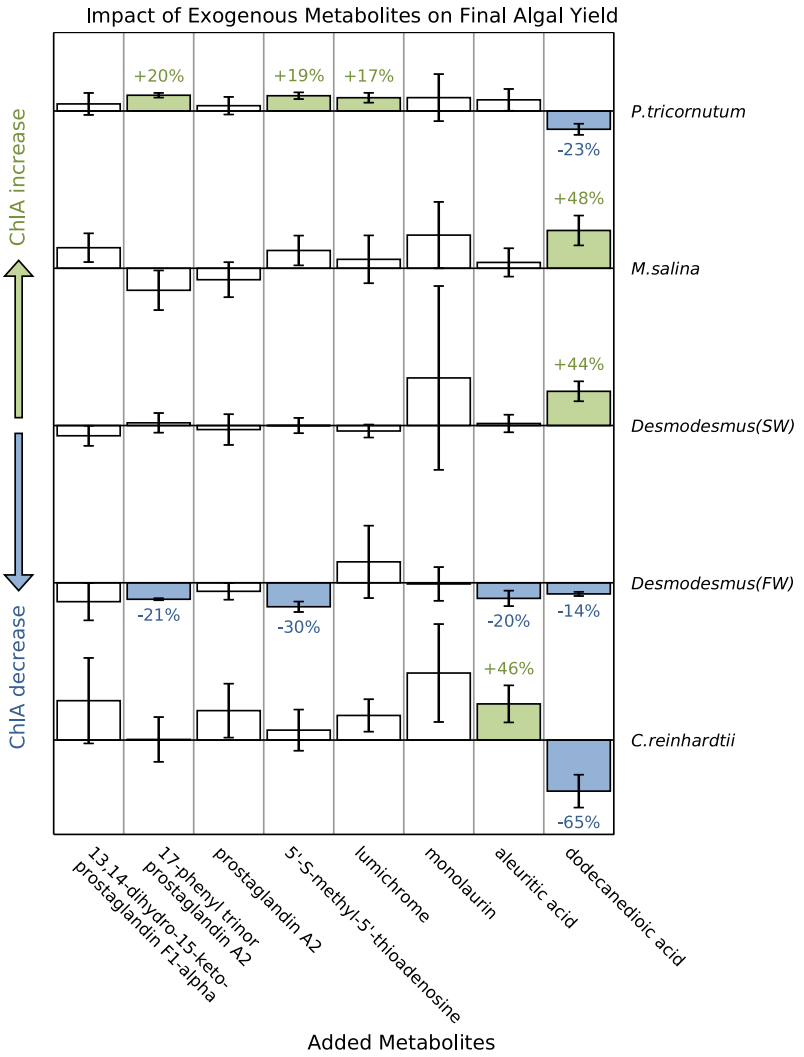

FIG 5 Impacts of select metabolites on algal growth as measured by chlorophyll A (ChlA) fluorescence. Bars and error bars show the averages and standard deviations of the increase or decrease of chlorophyll A fluorescence relative to controls of three biological replicates. Filled bars indicate a statistically significant decrease (blue) or increase (green), with the percent increase or decrease indicated above or below the bars.

dodecanedioic acid when grown in saltwater but negatively when grown in freshwater (14% decrease in chlorophyll A) (Fig. 5).

DISCUSSION

Our study builds on previous work to expand our understanding of microalgal exometabolome diversity, composition, and impacts on algal interactions. We set out to characterize exometabolomes from a phylogenetically and ecologically diverse set of microalgae, including two green algae (one freshwater, one freshwater and marine), a marine diatom, and a marine eustigmatophycean alga to discover exometabolites that may mediate algal interactions and ecophysiology. Given our interest in comparing algal responses to different salinities, we focused our analysis on nonpolar metabolites and used solid-phase extraction to minimize the influence of salinity on metabolite analysis. We find the following. (i) Exometabolite profiles are distinct between these eukaryotic microalgal strains, but we did not detect any correlation of exometabolomes with phylogeny among this limited number of strains. (ii) Based on the distinct responses to exogenous addition and salt and freshwater culturing, exometabolite

profiles may instead primarily reflect algal ecophysiology. (iii) Lumichrome, dipeptides, and prostaglandin-like compounds were enriched in the algal exometabolomes, none of which are well characterized in algal systems. (iv) Several compounds acted as effector metabolites, having significant impacts on algal growth. The exometabolites profiled may play roles in growth promotion, defense, and interactions as has been shown in other systems.

In our comparison across phylogenetically diverse algal strains, we found distinct metabolite profiles associated with each strain. Although we did observe matrix effects on the detection of internal controls (see Fig. S2 in the supplemental material), the fold changes for features between different cultures (median $\log_2$ fold change of -5.6) were much larger than the observed matrix effects (median $\log_2$ fold change of -0.15 to -2.0 for different sample groups) and can therefore be interpreted as real differences between metabolite levels in different cultures. One previous study has compared the exometabolomes of two cyanobacterial groups (three *Prochlorococcus* strains and two *Synechococcus* strain) with diatoms (two *Thalassosira* species and one *Phaeodactylum*) (16). That study found that the differences in the exometabolome profiles reflected the phylogenetic differences (prokaryote versus eukaryote) between these groups. Our results suggest that this phylogenetic signal is not consistently present within eukaryotic microalgae. *C. reinhardtii* and *Desmodesmus*, both members of the phylum Chlorophyta and class Chlorophyceae, are more closely related than the other strains used in our study (a diatom and an eustigmatophycean alga). However, their metabolite profiles did not cluster together in our analysis (Fig. 3, side dendrograms). Further, Mantel tests did not detect significant correlation between algal phylogenetic distance and exometabolome composition distance. A study of both macro- and microalgae found that environmental origin influenced intracellular metabolome composition more than phylogenetic relatedness (26). The results of our study suggest that exometabolite profiles are also not phylogenetically determined. However, because we studied only four algal strains, more work is needed to fully investigate the impact of phylogeny on microalgal exometabolomes.

The distinct profiles and responses of *Desmodesmus* under freshwater and saltwater conditions as well as the distinct responses of the microalgae to the exogenously added metabolites suggest that algal ecophysiology may be an important determinant of exudation. Given the signal suppression at high versus low salt concentrations that was observed in the analysis of the internal standards (even using solid-phase extraction) (Fig. S2), we focus on metabolites that increased with high salt. We find that *Desmodesmus* drastically shifts its exometabolome in response to salt- and freshwater culturing and has contrasting growth responses to addition of three of the eight tested metabolites under the different conditions, highlighting the responsiveness of the exometabolome to shifting environmental conditions. There have been some studies examining intracellular responses to different salinities by a variety of microalga, including *Scenedesmus* sp., *Amphora subtropica*, *Dunaliella* sp., *Desmodesmus armatus*, *Mesotaenium* sp., and *Tetraedron* sp. (27–30). Our work supports the finding that salinity impacts algal metabolite composition and extends it to the extracellular environment, suggesting that these differences will influence the surrounding community as well.

We assessed exometabolome enrichment as the ratio of exometabolome to cell pellet peak heights in paired samples. This ratio normalizes exometabolite peak heights to cell pellets and provides an estimate of exometabolome enrichment to enable identification of exometabolites of interest. However, this ratio is an imperfect approximation of enrichment. One limitation of this approach is that exometabolites accumulate over the course of the 8-day experiment, while endometabolites accumulate over the generation time of 1.3 to 2.4 days (estimated from algal growth data [Fig. 1]), with biomass concentrations increasing over time. Thus, the time scales of accumulation differ by a factor of approximately four. Because exometabolites are accumulating on the longer time scale, this may lead to an overestimate of enrichment based on this ratio.

Additionally, matrix effects, which can lower detection of metabolites in high salt samples (24, 25), differ between exometabolite and cell pellet samples, particularly for the saltwater cultures (Fig. S2). Saltwater exometabolite samples showed more signal suppression of internal standards than corresponding cell pellet samples. Thus, matrix effects also impact this ratio, biasing it toward an underestimate of enrichment, in the opposite direction from that expected for the potential time scale bias. Because of these uncertainties, it is important to note that this ratio is a qualitative measure of enrichment used to identify metabolites present at significant levels outside the cell. To minimize false-positive results in this analysis, we required enrichment ratios of at least two, in addition to statistical significance, to identify exometabolome-enriched metabolites in this analysis.

Several of the exometabolome-enriched metabolites may act as effector metabolites, with potentially important roles in algal growth and interactions with bacteria. Lumichrome (MSI identification level 1+), which was enriched in the exometabolomes of all cultures except *M. salina*, has been found to promote plant development and growth and has also been shown to impact bacterial quorum sensing (31, 32). *Chlamydomonas* is known to produce lumichrome (31), but lumichrome production has not been reported previously in *P. tricornutum* or *Desmodesmus*. Most previous studies of algae and lumichrome or riboflavin (vitamin B2), of which lumichrome is a derivative, have focused on possible lumichrome/riboflavin production by algal growth-promoting bacteria, as opposed to algal production (33–35). In addition to biological production, lumichrome can be produced through photochemical degradation of riboflavin (36). Since biomass concentrations were similar across the algal strains, it is unlikely that differences in light penetration could account for the observed differences in lumichrome accumulation. However, observed lumichrome levels likely represent a combination of direct biological production of lumichrome and photodegradation of biologically produced riboflavin. Because riboflavin was not detected in the exometabolomes, lumichrome and riboflavin levels could not be compared. Two recent studies found that exogenous lumichrome had positive growth impacts on the green algae *Chlorella sorokiniana* and *Auxenochlorella protothecoides* (33, 34), while another found that riboflavin increased chlorophyll production in *Chlorella vulgaris* (35). Supporting these studies, we found that *P. tricornutum*, which produced the highest level of lumichrome (Fig. S3), exhibited increased growth in response to exogenous lumichrome addition (Fig. 5), indicating it may be particularly important for this model diatom. To our knowledge, this is the first study showing impacts of lumichrome on a diatom or any saltwater microalga, expanding the range of systems where this compound may have important impacts. Further, given that lumichrome was enriched in four of the five exometabolomes and its role in bacterial quorum sensing, it could also play a role in modulating the phycosphere bacterial community.

Prostaglandin-like compounds were another group which were enriched in the exometabolomes of several of the algal strains (*C. reinhardtii*, *P. tricornutum*, and *M. salina*). Our data suggest that these features may represent related but novel compounds because these spectral matches were to unusual adducts or had a *m/z* error greater than 10 ppm. Prostaglandins are hormone-like signaling molecules found in a range of animals and plants (37–39). Originally discovered and studied in animals, prostaglandins have only recently been detected in microalgae, first being reported in the diatom *Skeletonema marinoi* (38). Although the roles of these compounds in microalgae have not yet been elucidated, these molecules are known to be involved in intracellular communication in other organisms. Prostaglandins have also been found to have diverse roles in marine macroalgae, including as defense molecules against pathogens in red macroalgae and as part of the oxidative response in brown macroalgae (37). A recent study in *P. tricornutum* detected the production of the isoprostanoids, which are structurally related to prostaglandins, under oxidative stress (40). That study found that the addition of 5 to 50 μM concentrations of several different isoprostanoids to *P. tricornutum* cultures decreased cell counts and increased lipid accumulation, while not

affecting photosynthetic efficiency. In comparison, we found that the addition of 10 μM 17-phenyl trinor prostaglandin A2 increased chlorophyll A production by *P. tricornutum* by 20% and decreased chlorophyll production of *Desmodesmus* grown in freshwater but not saltwater (Fig. 5). Interestingly, negative feature 13470, which showed spectral similarity to 17-phenyl trinor prostaglandin A2, was enriched in the exometabolome of *P. tricornutum*, but not that of *Desmodesmus* (Fig. 4). Together, these results suggest that prostaglandins and related compounds have important roles affecting microalgal growth.

Another interesting group of detected compounds included the di- and tripeptides, of which at least one was enriched in each of the five algal system exometabolomes profiled, indicating that this group of exometabolites is widespread across diverse microalgae. We identified one tripeptide and several dipeptides enriched in the alga exometabolomes, with specific dipeptides highly associated with either *P. tricornutum* or *C. reinhardtii* (Fig. S5). Dipeptides are known to be involved in interkingdom interactions as well as bacterial quorum sensing. For example, dipeptides have been implicated in coral-alga symbiosis (41, 42), as well as the interactions between land plants and arbuscular mychorhizal fungi (43). Cyclic dipeptides are important compounds for quorum sensing in Gram-positive bacteria and are also produced by other organisms to interfere with that quorum sensing (44). Linear dipeptides, like those detected in our study, have also been found to affect bacterial quorum sensing systems (45). The specificity of these dipeptides to particular algal taxa suggests that these metabolites may not be the result of general proteolysis but instead that these particular peptides may have important roles for these algae. Because these metabolites are enriched in the exometabolome, they could play a role in interkingdom interactions, as has been seen in these other systems.

The contrasting growth responses to exogenous addition of specific effector metabolites suggest there is delicate and distinct homeostasis with respect to these compounds and their extracellular and intracellular concentrations. Some metabolites are excreted to reduce toxicity but can also have growth promoting effects. Indole-3-acetic acid, a plant hormone also produced by some algae, stimulates growth of *Desmodesmus* at low concentrations but inhibits growth at concentrations above 200 μM (46). Contrasting growth responses of different algae to the same metabolite could also indicate allelopathy, in which one alga releases metabolites to inhibit competitors. In our study, negative feature 3830, with spectral similarity to the $[M\text{-}H\text{-}H_2O]^-$ adduct of aleuritic acid, was enriched in the exometabolomes of *C. reinhardtii*, *M. salina*, and *P. tricornutum*, but not in the exometabolome of *Desmodesmus* (Fig. 4). In the growth impact experiment, aleuritic acid inhibited the growth of *Desmodesmus* but not the other algae (Fig. 5). Interestingly, although features with spectral similarity to the $[M\text{-}H\text{-}H_2O]^-$ and $[M+H\text{-}3H_2O]^+$ adducts of dodecanedioic acid were enriched in the exometabolome of *P. tricornutum* (Fig. 4), the addition of 0.01 mM dodecanedioic acid significantly inhibited *P. tricornutum* growth (Fig. 5). However, this inhibition was concentration dependent, with the lowest concentration tested (0.0001 mM) slightly increasing growth (Fig. S6). This result suggests that overaccumulation of some exometabolites could result in self inhibition.

There are some limitations to this study which are important to consider. First, our analysis has focused on nonpolar C_{18} extractable metabolites, which enabled analysis of changes in response to salt concentration and analysis of compounds relevant to signaling. However, excluding polar metabolites provides a limited view of overall exudates. Because the extraction method is biased toward and against certain groups of metabolites and because the presence of other metabolites can affect extraction, extraction efficiencies can vary depending on the metabolite composition of the sample. We did not measure extraction efficiencies in our study, but a previous study of estuarian water estimated a dissolved organic matter extraction efficiency of 23% to 27% for the solid-phase extraction columns used in our study (47), while another study found that extraction efficiencies for a different C_{18} extraction column ranged from 35% to 45% between deep sea and estuarian samples (48). These represent much

TABLE 1 Growth media, organisms, and strain information for algal growth experiments

Medium	Organism	Strain
Freshwater (Bristol's medium)	*Chlamydomonas reinhardtii*	CC-1690
	Desmodesmus sp.	C046
Saltwater (ESAW medium)	*Phaeodactylum tricornutum*	CCMP 2561
	Microchloropsis salina	CCMP 1776
	Desmodesmus sp.	C046

smaller differences (log_2 fold change = 0.2 to 0.4) than were observed between sample groups in our study (median log_2 fold change = −5.6 across features). Extraction efficiencies of individual compounds or compound classes of interest may be more relevant to consider for these comparisons than overall organic matter extraction efficiency. Johnson et al. found that extraction efficiencies varied across a suite of isotopically labeled spiked-in metabolite standards between marine cultures (49). The fold changes in extraction efficiencies between cultures observed in that study were small (median log_2 fold change of 0.5) compared to those observed in our data. Unfortunately, determination of extraction efficiencies for individual metabolites of interest, which were unknown at the outset of our study, was not feasible for this exploratory untargeted study. Differences in extractions are also an important consideration when relating these results to previous algal metabolomics studies. For instance, other studies of algal exometabolites have used different solid-phase extraction protocols (e.g., to target small polar molecules) (11, 15) or derivatize samples prior to extraction (15). Known differences in extraction protocols should be considered when comparing our study, which focuses on nonpolar C_{18} extractable metabolites, to other studies with different focuses. A second limitation of this study is that, given our focus on diverse nonpolar metabolites, relatively few were identified. Therefore, an important future direction will be the extension of this work to the analysis of polar metabolites which include many well-characterized molecules such as sugars, amino acids, and small organic acids. Further, given the large phylogenetic distances and limited number of taxa profiled, there are some limitations to what can be concluded about phylogenetic correlations and the specificity of exometabolites to phyla. However, because of the wide diversity of the algal systems studied, the similarities provide evidence for exometabolites that are commonly exuded by microalgae.

This work adds to our understanding of microalgal exometabolomes. We found that variation in eukaryotic microalgal exometabolome composition is not primarily phylogenetically driven and is affected by growth conditions. We also identified impacts of specific effector metabolites, many of which have not been identified or characterized in algae, on algal growth. Further work is now needed to understand the roles of these metabolites in more complex algal-bacterial systems and to extend this work to include polar metabolites.

MATERIALS AND METHODS

Algal strains and growth conditions. This study used four microalgal strains, as detailed in Table 1. Two of the algal strains (*C. reinhardtii* and *Desmodesmus*) were grown in freshwater medium, and three (*P. tricornutum*, *M. salina*, and *Desmodesmus*) were grown in saltwater medium.

Saltwater growth medium was prepared using salts for enriched saltwater artificial water (ESAW) medium (50, 51). Saltwater medium contained 21.194 g/liter NaCl, 3.55 g/liter Na_2SO_4, 0.599 g/liter KCl, 0.174 g/liter $NaHCO_3$, 0.0863 g/liter KBr, 0.023 g/liter H_3PO_4, 0.0028 g/liter NaF, 9.592 g/liter $MgCl_2{\cdot}6H_2O$, 1.344 g/liter $CaCl_2{\cdot}2H_2O$, 0.0218 g/liter $SrCl_2{\cdot}6H_2O$, and 0.03 g/liter $Na_2SiO_3{\cdot}9H_2O$. Additionally, nitrate, phosphate, trace metals, and vitamins were added at the concentrations for F/2 medium (52). Nitrate and phosphate were added as 0.075 g/liter $NaNO_3$ and 0.005 g/liter $NaH_2PO_4{\cdot}H_2O$, respectively. The final concentrations of trace metals were 0.023 mg/liter $ZnSO_4{\cdot}7H_2O$, 0.152 mg/liter $MnSO_4{\cdot}H_2O$, 0.0073 mg/liter $NaMoO_4{\cdot}2H_2O$, 0.014 mg/liter $CoSO_4{\cdot}7H_2O$, 0.0068 mg/liter $CuCl_2{\cdot}2H_2O$, 4.6 mg/liter $Fe(NH_4)_2(SO_4)_2{\cdot}6H_2O$, and 4.4 mg/liter $Na_2EDTA{\cdot}2H_2O$. Vitamin final

concentrations were 0.0135 mg/liter cyanocobalamin (vitamin B12), 0.0025 mg/liter biotin, and 0.0335 mg/liter thiamine.

Freshwater medium was prepared based on Bristol's medium. Bristol's medium contained 0.025 g/liter NaCl, 0.025 g/liter $CaCl_2 \cdot 2H_2O$, 0.075 g/liter $MgSO_4 \cdot 7H_2O$, 0.25g $NaNO_3$, 0.075g/liter K_2HPO_4, and 0.175 g/liter KH_2PO_4. To make the freshwater and saltwater conditions more comparable, the same F/2 levels of trace metals and vitamins listed above for saltwater medium were also added to the freshwater medium.

Algae were grown in glass 125-ml Erlenmeyer flasks that had previously been baked in a muffle furnace at 550°C for 2 h to remove trace organics that could contaminate metabolomics analyses. Each flask contained 50 ml of the appropriate medium and was capped with a foam stopper and covered with aluminum foil to avoid contamination during the experiment. Flasks were incubated with shaking at 90 rpm in a light incubator, with a 12-h day/night light cycle. Daytime illumination was 3,500 lx, and the incubator temperature was maintained at 22°C. Algal inocula were prepared by first growing algal stock cultures under experimental conditions (flasks, media, incubation) for 1 week to acclimate cultures to those conditions. After 7 days, experimental flasks were inoculated by transferring 2 ml of inoculum culture to flasks with the appropriate medium. Twenty-five biological replicate cultures were prepared for each algal and control condition to allow destructive sampling of five replicates at each sampling time point (0, 4, 8, 12, and 18 days).

Sample collection. Chlorophyll A measurement samples were collected by transferring 1 ml of culture to a clear 5-ml polystyrene tube. Microscopy samples were collected by transferring a 1-ml sample from the flask to a 1.5-ml microcentrifuge tube, adding 100 μl of formaldehyde to fix cells, and storing the sample at 4°C until performing microscopy to determine the axenicity of the culture.

After removal of samples for chlorophyll measurements and microscopy, the remainder of the culture was destructively harvested to collect cell pellets and spent medium. Spent medium and cell pellets were separated by centrifugation. Half of the culture was transferred to a 50-ml Falcon tube and centrifuged at 5,000 $\times$ *g* for 8 min at 4°C. The supernatant was carefully transferred to a clean Falcon tube, the remainder of the culture was added to the tube containing the pellet, and the centrifugation procedure was repeated. After separation by centrifugation, the supernatant was filtered through a 0.45-μm-pore-size syringe filter to remove residual algal cells. Filtered spent medium and cell pellets were frozen on dry ice and stored at −80°C until extraction.

To disrupt cells for metabolite extraction, cell pellets were resuspended in 1-ml sterile water, frozen at −80°C, and lyophilized. Lyophilized pellets were disrupted using a sterilized steel ball and vortexing three times for 5 s. Disrupted pellets were then resuspended in 50-ml sterile water and filtered and frozen in the same manner as spent medium. Thus, the spent medium and cell pellet samples corresponded to the same original sample volume.

Chlorophyll A fluorescence, biomass, and organic carbon measurements. Chlorophyll A fluorescence of samples from flask grow cultures was measured using a Trilogy fluorometer (Turner Designs, San Jose, CA, USA) with the Chlorophyll A In-Vivo Module.

Biomass was measured as the ash-free dry weight of the cell pellets collected on days 4 and 8. Cell pellets were transferred to aluminum dishes and dried at 95°C overnight. The dry weight of the pellet and aluminum dish was measured. Pellets were then ashed at 500°C for 4 h, and the weight of the remaining ash and aluminum dish was measured. Ash-free dry weight was calculated as the difference between the two measured weights.

Samples were prepared for total organic carbon (TOC) measurement by diluting 1.4-ml sample (spent medium or cell pellet extract) with 5.6-ml ultrapure water for a 1:5 dilution. TOC was measured on a Shimadzu TOC analyzer.

Metabolite profiling. Samples for LC-MS/MS metabolomics analysis were extracted by solid-phase extraction using Waters Sep-Pak C_{18} 3-ml cartridges. Because chlorophyll and biomass content were similar across samples, samples were normalized to the same volume (30 ml). Cartridges were first preconditioned with 3 ml of methanol and then rinsed with 6 ml of ultrapure water. Metabolites were extracted by passing 30 ml of sample through the cartridge. Columns with extracted metabolites were rinsed with 6 ml of ultrapure water. Metabolites were eluted with 1 ml of methanol into a 1.5-ml polypropylene tube and then dried in a vacuum centrifuge with a refrigerated vapor trap.

Dried metabolite extracts were prepared for analysis as previously described (9, 53, 54). Briefly, samples were resuspended in 150 μl of methanol with ^{13}C- and ^{15}N-labeled matrix control internal standards (see Table S2 in the supplemental material), vortexed for 5 to 10 s, and sonicated in a water bath sonicator with ice for 10 min. Resuspension in 150 μl of methanol was performed to obtain more concentrated extracts for analysis, and internal standards were used to evaluate matrix effects, which can impact metabolite detection (55). Samples were centrifuged at 10,000 $\times$ *g* for 5 min at 4°C to pellet insoluble salts and proteins. Supernatant was transferred to a 0.2-μm-pore-size centrifuge filter device and centrifuged at 5,000 $\times$ *g* for 5 min at 4°C. Filtrate was transferred to an autosampler vial for LC-MS/MS analysis.

LC-MS/MS was performed as previously described (56), and the LC gradient and MS conditions are provided in Table S2. Briefly, chromatographic separation of metabolites in samples were performed using reverse-phase liquid chromatography on a Zorbax EclipsePlusC18 RRHD 1.8 μm, 2.1 $\times$ 50 mm column (Agilent Technologies, Santa Clara, CA, USA) on an Agilent 1290 series ultra high-performance LC system. Mass spectrometry analyses were performed using a Thermo Fisher Scientific Q Exactive Hybrid Quadrupole-Orbitrap mass spectrometer (Thermo Fisher Scientific, Waltham, MA, USA). LCMS parameters used for analysis are defined in Table S2.

Untargeted analysis of LC-MS/MS data was performed to identify metabolites as previously described (56). Briefly, LC-MS/MS features, corresponding to specific retention time and *m/z* combinations, were detected using the MZMine software v. 2.53 (57, 58). Detected features were analyzed using the Global Natural Products Social Molecular Networking tool (GNPS) to construct feature-based molecular networks (20, 21). This analysis creates networks of potentially related features, using spectral similarity as a proxy for structural similarity. Preliminary feature annotations were determined based on the highest scoring MS2 match to the GNPS database. For features identified as statistically significant in subsequent analyses, putative annotations were made by hand curation of the top 100 matches to the GNPS database, based on GNPS cosine score, delta *m/z*, number of shared peaks, and common adducts.

Impacts of select metabolites on algae. Impacts of selected metabolites on algal chlorophyll A production were tested in 48-well plates. Each metabolite was tested individually for each of the algal strains at concentrations of 0.01, 0.001, and 0.0001 mM. The highest concentration of 0.01 mM was selected based on a previous study of the impacts of phytohormones on *C. reinhardtii* growth (5). Each well contained 750 μl of media with or without added metabolite and was inoculated with 15 μl of 1-week-old algal inoculum. Each metabolite was tested for each alga in triplicate in randomly positioned wells. Plates were incubated with a 12-h light/dark cycle for 12 days with shaking at 90 rpm. Chlorophyll A fluorescence of plate growth assays was measured in a Cytation5 plate reader (BioTek, Winooski, VT, USA) with excitation and emission wavelengths of 440 nm and 680 nm, respectively.

Statistical analyses. LC/MS-MS features significantly different from background were identified by comparing feature peak heights for test samples to those of medium blanks with two-tailed *t* tests and using the Bonferroni correction to account for multiple comparisons. Features were considered significant if at least one sample group had an adjusted *P* value of <0.05 and at least twofold above the signal in control samples.

Features significantly enriched in the exometabolome were identified by first calculating the ratio of the peak heights for paired exometabolome and pellet metabolome samples. A one-sample *t* test was used to compare mean of the base two logarithm of these ratios to zero, using the Benjamini-Hochberg adjustment to correct for multiple comparisons. A feature was considered significantly exometabolome enriched for a particular alga if the adjusted *P* value was less than 0.05 and average ratio of extracellular to cell pellet peak height was at least 2.

Mantel tests were conducted using the "mantel" function in the "vegan" package v. 2.5-7 in R v. 4.0.5. Phylogenetic distances were calculated based on multiple sequence alignment of 18S rRNA genes to the global SILVA alignment for rRNA genes (59). Metabolome distance matrices were determined based on Euclidean distances of normalized metabolite profiles. Separate Mantel tests were performed using either the freshwater or saltwater exometabolomes for *Desmodesmus* in the metabolome distance matrix.

Data availability. LC-MS/MS raw data and metadata are available at the NIH Common Fund's National Metabolomics Data Repository (NMDR) (supported by NIH grant U2C-DK119886) website, the Metabolomics Workbench at https://www.metabolomicsworkbench.org where it has been assigned project identifier (ID) PR001206. The data can be accessed directly via its project doi (https://doi.org/10.21228/M8TD6R). GNPS molecular networks and preliminary spectral matches are available at https://gnps.ucsd.edu/ProteoSAFe/status.jsp?task=29549d19521944368add9234d215fa1b and https://gnps.ucsd.edu/ProteoSAFe/status.jsp?task=f14b47591e6c40aab59907aa2f631059. The GNPS expanded spectral matches used for curation of feature annotations are available at https://gnps.ucsd.edu/ProteoSAFe/status.jsp?task=42f8bb1af9f74575b985da04fd1e6c77 and https://gnps.ucsd.edu/ProteoSAFe/status.jsp?task=19fd0e195daa481893aa7e6f93de4573.

SUPPLEMENTAL MATERIAL

Supplemental material is available online only.

DATA SET S1, XLSX file, 10.4 MB.

FIG S1, PDF file, 0.03 MB.

FIG S2, PDF file, 0.05 MB.

FIG S3, PDF file, 0.04 MB.

FIG S4, PDF file, 1 MB.

FIG S5, PDF file, 0.04 MB.

FIG S6, PDF file, 0.03 MB.

FIG S7, PDF file, 0.03 MB.

TABLE S1, XLSX file, 0.04 MB.

TABLE S2, XLSX file, 0.01 MB.

ACKNOWLEDGMENTS

This research was supported by the LLNL Biofuels Scientific Focus Area, funded by the U.S. Department of Energy Office of Science, Office of Biological and Environmental Research Genomic Science program under FWP SCW1039. This work was performed under the auspices of the U.S. Department of Energy by Lawrence Livermore National

Laboratory under contract DE-AC52-07NA27344. The LLNL IM release number was LLNL-JRNL-823908.

REFERENCES

1. Falkowski P. 2012. Ocean science: the power of plankton. Nature 483: S17–S20. https://doi.org/10.1038/483S17a.
2. Chisti Y. 2007. Biodiesel from microalgae. Biotechnol Adv 25:294–306. https://doi.org/10.1016/j.biotechadv.2007.02.001.
3. Mata TM, Martins AA, Caetano NS. 2010. Microalgae for biodiesel production and other applications: a review. Renew Sustain Energy Rev 14: 217–232. https://doi.org/10.1016/j.rser.2009.07.020.
4. Cirri E, Pohnert G. 2019. Algae-bacteria interactions that balance the planktonic microbiome. New Phytol 223:100–106. https://doi.org/10.1111/nph.15765.
5. Park WK, Yoo G, Moon M, Kim C, Choi YE, Yang JW. 2013. Phytohormone supplementation significantly increases growth of Chlamydomonas reinhardtii cultivated for biodiesel production. Appl Biochem Biotechnol 171: 1128–1142. https://doi.org/10.1007/s12010-013-0386-9.
6. Labeeuw L, Khey J, Bramucci AR, Atwal H, de la Mata AP, Harynuk J, Case RJ. 2016. Indole-3-acetic acid is produced by Emiliania huxleyi coccolith-bearing cells and triggers a physiological response in bald cells. Front Microbiol 7:828. https://doi.org/10.3389/fmicb.2016.00828.
7. Leflaive J, Lacroix G, Nicaise Y, Ten-Hage L. 2008. Colony induction and growth inhibition in Desmodesmus quadrispina (Chlorococcales) by allelochemicals released from the filamentous alga Uronema confervicolum (Ulotrichales). Environ Microbiol 10:1536–1546. https://doi.org/10.1111/j.1462-2920.2008.01569.x.
8. Seymour JR, Amin SA, Raina JB, Stocker R. 2017. Zooming in on the phycosphere: the ecological interface for phytoplankton-bacteria relationships. Nat Microbiol 2:12. https://doi.org/10.1038/nmicrobiol.2017.65.
9. Zhalnina K, Louie KB, Hao Z, Mansoori N, da Rocha UN, Shi SJ, Cho HJ, Karaoz U, Loque D, Bowen BP, Firestone MK, Northen TR, Brodie EL. 2018. Dynamic root exudate chemistry and microbial substrate preferences drive patterns in rhizosphere microbial community assembly. Nat Microbiol 3:470–480. https://doi.org/10.1038/s41564-018-0129-3.
10. Fu H, Uchimiya M, Gore J, Moran MA. 2020. Ecological drivers of bacterial community assembly in synthetic phycospheres. Proc Natl Acad Sci U S A 117:3656–3662. https://doi.org/10.1073/pnas.1917265117.
11. Shibl AA, Isaac A, Ochsenkuhn MA, Cardenas A, Fei C, Behringer G, Arnoux M, Drou N, Santos MP, Gunsalus KC, Voolstra CR, Amin SA. 2020. Diatom modulation of select bacteria through use of two unique secondary metabolites. Proc Natl Acad Sci U S A 117:27445–27455. https://doi.org/10.1073/pnas.2012088117.
12. Seyedsayamdost MR, Wang RR, Kolter R, Clardy J. 2014. Hybrid biosynthesis of roseobacticides from algal and bacterial precursor molecules. J Am Chem Soc 136:15150–15153. https://doi.org/10.1021/ja508782y.
13. Remmers IM, D'Adamo S, Martens DE, de Vos RCH, Mumm R, America AHP, Cordewener JHG, Bakker LV, Peters SA, Wijffels RH, Lamers PP. 2018. Orchestration of transcriptome, proteome and metabolome in the diatom Phaeodactylum tricornutum during nitrogen limitation. Algal Res 35: 33–49. https://doi.org/10.1016/j.algal.2018.08.012.
14. Bolling C, Fiehn O. 2005. Metabolite profiling of Chlamydomonas reinhardtii under nutrient deprivation. Plant Physiol 139:1995–2005. https://doi.org/10.1104/pp.105.071589.
15. Ferrer-González FX, Widner B, Holderman NR, Glushka J, Edison AS, Kujawinski EB, Moran MA. 2021. Resource partitioning of phytoplankton metabolites that support bacterial heterotrophy. ISME J 15:762–773. https://doi.org/10.1038/s41396-020-00811-y.
16. Becker JW, Berube PM, Follett CL, Waterbury JB, Chisholm SW, DeLong EF, Repeta DJ. 2014. Closely related phytoplankton species produce similar suites of dissolved organic matter. Front Microbiol 5:111. https://doi.org/10.3389/fmicb.2014.00111.
17. Baran R, Bowen BP, Northen TR. 2011. Untargeted metabolic footprinting reveals a surprising breadth of metabolite uptake and release by Synechococcus sp. PCC 7002. Mol Biosyst 7:3200–3206. https://doi.org/10.1039/c1mb05196b.
18. Merchant SS, Prochnik SE, Vallon O, Harris EH, Karpowicz SJ, Witman GB, Terry A, Salamov A, Fritz-Laylin LK, Marechal-Drouard L, Marshall WF, Qu LH, Nelson DR, Sanderfoot AA, Spalding MH, Kapitonov VV, Ren QH, Ferris P, Lindquist E, Shapiro H, Lucas SM, Grimwood J, Schmutz J, Cardol P, Cerutti H, Chanfreau G, Chen CL, Cognat V, Croft MT, Dent R, Dutcher S, Fernandez E, Fukuzawa H, Gonzalez-Ballester D, Gonzalez-Halphen D, Hallmann A, Hanikenne M, Hippler M, Inwood W, Jabbari K, Kalanon M, Kuras R, Lefebvre PA, Lemaire SD, Lobanov AV, Lohr M, Manuell A, Meir I, Mets L, Mittag M, et al. 2007. The Chlamydomonas genome reveals the evolution of key animal and plant functions. Science 318:245–251. https://doi.org/10.1126/science.1143609.
19. Bowler C, Allen AE, Badger JH, Grimwood J, Jabbari K, Kuo A, Maheswari U, Martens C, Maumus F, Otillar RP, Rayko E, Salamov A, Vandepoele K, Beszteri B, Gruber A, Heijde M, Katinka M, Mock T, Valentin K, Verret F, Berges JA, Brownlee C, Cadoret JP, Chiovitti A, Choi CJ, Coesel S, De Martino A, Detter JC, Durkin C, Falciatore A, Fournet J, Haruta M, Huysman MJJ, Jenkins BD, Jiroutova K, Jorgensen RE, Joubert Y, Kaplan A, Kroger N, Kroth PG, La Roche J, Lindquist E, Lommer M, Martin-Jezequel V, Lopez PJ, Lucas S, Mangogna M, McGinnis K, Medlin LK, Montsant A, et al. 2008. The Phaeodactylum genome reveals the evolutionary history of diatom genomes. Nature 456:239–244. https://doi.org/10.1038/nature07410.
20. Nothias LF, Petras D, Schmid R, Duhrkop K, Rainer J, Sarvepalli A, Protsyuk I, Ernst M, Tsugawa H, Fleischauer M, Aicheler F, Aksenov AA, Alka O, Allard PM, Barsch A, Cachet X, Caraballo-Rodriguez AM, Da Silva RR, Dang T, Garg N, Gauglitz JM, Gurevich A, Isaac G, Jarmusch AK, Kamenik Z, Kang KB, Kessler N, Koester I, Korf A, Le Gouellec A, Ludwig M, Martin HC, McCall LI, McSayles J, Meyer SW, Mohimani H, Morsy M, Moyne O, Neumann S, Neuweger H, Nguyen NH, Nothias-Esposito M, Paolini J, Phelan VV, Pluskal T, Quinn RA, Rogers S, Shrestha B, Tripathi A, van der Hooft JJJ, et al. 2020. Feature-based molecular networking in the GNPS analysis environment. Nat Methods 17:905–908. https://doi.org/10.1038/s41592-020-0933-6.
21. Wang M, Carver JJ, Phelan VV, Sanchez LM, Garg N, Peng Y, Nguyen DD, Watrous J, Kapono CA, Luzzatto-Knaan T, Porto C, Bouslimani A, Melnik AV, Meehan MJ, Liu W-T, Crüsemann M, Boudreau PD, Esquenazi E, Sandoval-Calderón M, Kersten RD, Pace LA, Quinn RA, Duncan KR, Hsu C-C, Floros DJ, Gavilan RG, Kleigrewe K, Northen T, Dutton RJ, Parrot D, Carlson EE, Aigle B, Michelsen CF, Jelsbak L, Sohlenkamp C, Pevzner P, Edlund A, McLean J, Piel J, Murphy BT, Gerwick L, Liaw C-C, Yang Y-L, Humpf H-U, Maansson M, Keyzers RA, Sims AC, Johnson AR, Sidebottom AM, Sedio BE, et al. 2016. Sharing and community curation of mass spectrometry data with Global Natural Products Social Molecular Networking. Nat Biotechnol 34:828–837. https://doi.org/10.1038/nbt.3597.
22. Fiehn O, Robertson D, Griffin J, van der Werf M, Nikolau B, Morrison N, Sumner LW, Goodacre R, Hardy NW, Taylor C, Fostel J, Kristal B, Kaddurah-Daouk R, Mendes P, van Ommen B, Lindon JC, Sansone SA. 2007. The metabolomics standards initiative (MSI). Metabolomics 3:175–178. https://doi.org/10.1007/s11306-007-0070-6.
23. Sumner LW, Amberg A, Barrett D, Beale MH, Beger R, Daykin CA, Fan TWM, Fiehn O, Goodacre R, Griffin JL, Hankemeier T, Hardy N, Harnly J, Higashi R, Kopka J, Lane AN, Lindon JC, Marriott P, Nicholls AW, Reily MD, Thaden JJ, Viant MR. 2007. Proposed minimum reporting standards for chemical analysis. Metabolomics 3:211–221. https://doi.org/10.1007/s11306-007-0082-2.
24. Alvarez-Sanchez B, Priego-Capote F, de Castro MDL. 2010. Metabolomics analysis II. Preparation of biological samples prior to detection. TrAC Trends Anal Chem 29:120–127. https://doi.org/10.1016/j.trac.2009.12.004.
25. Pontrelli S, Sauer U. 2021. Salt-tolerant metabolomics for exometabolomic measurements of marine bacterial isolates. Anal Chem 93:7164–7171. https://doi.org/10.1021/acs.analchem.0c04795.
26. Hughes AH, Magot F, Tawfike AF, Rad-Menendez C, Thomas N, Young LC, Stucchi L, Carettoni D, Stanley MS, Edrada-Ebel R, Duncan KR. 2021. Exploring the chemical space of macro- and micro-algae using comparative metabolomics. Microorganisms 9:311. https://doi.org/10.3390/microorganisms9020311.
27. Arora N, Kumari P, Kumar A, Gangwar R, Gulati K, Pruthi PA, Prasad R, Kumar D, Pruthi V, Poluri KM. 2019. Delineating the molecular responses of a halotolerant microalga using integrated omics approach to identify genetic engineering targets for enhanced TAG production. Biotechnol Biofuels 12:2. https://doi.org/10.1186/s13068-018-1343-1.
28. Arora N, Laurens LML, Sweeney N, Pruthi V, Poluri KM, Pienkos PT. 2019. Elucidating the unique physiological responses of halotolerant Scenedesmus

sp. cultivated in sea water for biofuel production. Algal Res 37:260–268. https://doi.org/10.1016/j.algal.2018.12.003.
29. BenMoussa-Dahmen I, Chtourou H, Rezgui F, Sayadi S, Dhouib A. 2016. Salinity stress increases lipid, secondary metabolites and enzyme activity in Amphora subtropica and Dunaliella sp. for biodiesel production. Bioresour Technol 218:816–825. https://doi.org/10.1016/j.biortech.2016.07.022.
30. von Alvensleben N, Magnusson M, Heimann K. 2016. Salinity tolerance of four freshwater microalgal species and the effects of salinity and nutrient limitation on biochemical profiles. J Appl Phycol 28:861–876. https://doi.org/10.1007/s10811-015-0666-6.
31. Rajamani S, Bauer WD, Robinson JB, Farrow JM, Pesci EC, Teplitski M, Gao MS, Sayre RT, Phillips DA. 2008. The vitamin riboflavin and its derivative lumichrome activate the LasR bacterial quorum-sensing receptor. Mol Plant Microbe Interact 21:1184–1192. https://doi.org/10.1094/MPMI-21-9-1184.
32. Dakora FD, Matiru VN, Kanu A. 2015. Rhizosphere ecology of lumichrome and riboflavin, two bacterial signal molecules eliciting developmental changes in plants. Front Plant Sci 6:11. https://doi.org/10.3389/fpls.2015.00700.
33. Lopez BR, Palacios OA, Bashan Y, Hernandez-Sandoval FE, de-Bashan LE. 2019. Riboflavin and lumichrome exuded by the bacterium Azospirillum brasilense promote growth and changes in metabolites in Chlorella sorokiniana under autotrophic conditions. Algal Res 44:101696. https://doi.org/10.1016/j.algal.2019.101696.
34. Peng HX, de-Bashan LE, Higgins BT. 2021. Comparison of algae growth and symbiotic mechanisms in the presence of plant growth promoting bacteria and non-plant growth promoting bacteria. Algal Res 53:102156. https://doi.org/10.1016/j.algal.2020.102156.
35. Heo J, Kim S, Cho DH, Song GC, Kim HS, Ryu CM. 2019. Genome-wide exploration of Escherichia coli genes to promote Chlorella vulgaris growth. Algal Res 38:101390. https://doi.org/10.1016/j.algal.2018.101390.
36. Ahmad I, Fasihullah Q, Noor A, Ansari IA, Ali QNM. 2004. Photolysis of riboflavin in aqueous solution: a kinetic study. Int J Pharm 280:199–208. https://doi.org/10.1016/j.ijpharm.2004.05.020.
37. Di Costanzo F, Di Dato V, Ianora A, Romano G. 2019. Prostaglandins in marine organisms: a review. Marine Drugs 17:428. https://doi.org/10.3390/md17070428.
38. Di Dato V, Orefice I, Amato A, Fontanarosa C, Amoresano A, Cutignano A, Ianora A, Romano G. 2017. Animal-like prostaglandins in marine microalgae. ISME J 11:1722–1726. https://doi.org/10.1038/ismej.2017.27.
39. Groenewald EG, van der Westhuizen AJ. 1997. Prostaglandins and related substances in plants. Bot Rev 63:199–220. https://doi.org/10.1007/BF02857948.
40. Lupette J, Jaussaud A, Vigor C, Oger C, Galano JM, Reversat G, Vercauteren J, Jouhet J, Durand T, Marechal E. 2018. Non-enzymatic synthesis of bioactive isoprostanoids in the diatom Phaeodactylum following oxidative stress. Plant Physiol 178:1344–1357. https://doi.org/10.1104/pp.18.00925.
41. Williams A, Chiles EN, Conetta D, Pathmanathan JS, Cleves PA, Putnam HM, Su XY, Bhattacharya D. 2021. Metabolomic shifts associated with heat stress in coral holobionts. Sci Adv 7:9. https://doi.org/10.1126/sciadv.abd4210.
42. Verbeke F, De Craemer S, Debunne N, Janssens Y, Wynendaele E, Van de Wiele C, De Spiegeleer B. 2017. Peptides as quorum sensing molecules: measurement techniques and obtained levels in vitro and in vivo. Front Neurosci 11:183–118. https://doi.org/10.3389/fnins.2017.00183.
43. Belmondo S, Fiorilli V, Perez-Tienda J, Ferrol N, Marmeisse R, Lanfranco L. 2014. A dipeptide transporter from the arbuscular mycorrhizal fungus Rhizophagus irregularis is upregulated in the intraradical phase. Front Plant Sci 5:436. https://doi.org/10.3389/fpls.2014.00436.
44. Holden MTG, Chhabra SR, de Nys R, Stead P, Bainton NJ, Hill PJ, Manefield M, Kumar N, Labatte M, England D, Rice S, Givskov M, Salmond GPC, Stewart G, Bycroft BW, Kjelleberg SA, Williams P. 1999. Quorum-sensing cross talk: isolation and chemical characterization of cyclic dipeptides from Pseudomonas aeruginosa and other Gram-negative bacteria. Mol Microbiol 33:1254–1266. https://doi.org/10.1046/j.1365-2958.1999.01577.x.
45. Naik DN, Wahidullah S, Meena RM. 2013. Attenuation of Pseudomonas aeruginosa virulence by marine invertebrate derived Streptomyces sp. Lett Appl Microbiol 56:197–207. https://doi.org/10.1111/lam.12034.
46. Chung TY, Kuo CY, Lin WJ, Wang WL, Chou JY. 2018. Indole-3-acetic-acid-induced phenotypic plasticity in Desmodesmus algae. Sci Rep 8:13. https://doi.org/10.1038/s41598-018-28627-z.
47. Mills GL, McFadden E, Quinn JG. 1987. Chromatographic studies of dissolved organic-matter and copper organic-complexes isolated from estuarine waters. Marine Chem 20:313–325. https://doi.org/10.1016/0304-4203(87)90065-X.
48. Dittmar T, Koch B, Hertkorn N, Kattner G. 2008. A simple and efficient method for the solid-phase extraction of dissolved organic matter (SPE-DOM) from seawater. Limnol Oceanogr Methods 6:230–235. https://doi.org/10.4319/lom.2008.6.230.
49. Johnson WM, Soule MCK, Kujawinski EB. 2017. Extraction efficiency and quantification of dissolved metabolites in targeted marine metabolomics. Limnol Oceanogr Methods 15:417–428. https://doi.org/10.1002/lom3.10181.
50. Berges JA, Franklin DJ, Harrison PJ. 2001. Evolution of an artificial seawater medium: improvements in enriched seawater, artificial water over the last two decades. J Phycol 37:1138–1145. https://doi.org/10.1046/j.1529-8817.2001.01052.x.
51. Harrison PJ, Waters RE, Taylor FJR. 1980. A broad-spectrum artificial seawater medium for coastal and open ocean phytoplankton. J Phycol 16:28–35. https://doi.org/10.1111/j.0022-3646.1980.00028.x.
52. Guillard RR, Ryther JH. 1962. Studies of marine planktonic diatoms.1. Cyclotella nana Hustedt, and Detonula confervacea (Cleve) Gran. Can J Microbiol 8:229–239. https://doi.org/10.1139/m62-029.
53. Swift CL, Louie KB, Bowen BP, Olson HM, Purvine SO, Salamov A, Mondo SJ, Solomon KV, Wright AT, Northen TR, Grigoriev IV, Keller NP, O'Malley MA. 2021. Anaerobic gut fungi are an untapped reservoir of natural products. Proc Natl Acad Sci U S A 118:e2019855118. https://doi.org/10.1073/pnas.2019855118.
54. Malik AA, Swenson T, Weihe C, Morrison EW, Martiny JBH, Brodie EL, Northen TR, Allison SD. 2020. Drought and plant litter chemistry alter microbial gene expression and metabolite production. ISME J 14:2236–2247. https://doi.org/10.1038/s41396-020-0683-6.
55. Boysen AK, Heal KR, Carlson LT, Ingalls AE. 2018. Best-matched internal standard normalization in liquid chromatography-mass spectrometry metabolomics applied to environmental samples. Anal Chem 90:1363–1369. https://doi.org/10.1021/acs.analchem.7b04400.
56. Murphy KM, Edwards J, Louie KB, Bowen BP, Sundaresan V, Northen TR, Zerbe P. 2021. Bioactive diterpenoids impact the composition of the root-associated microbiome in maize (Zea mays). Sci Rep 11:13. https://doi.org/10.1038/s41598-020-79320-z.
57. Katajamaa M, Miettinen J, Oresic M. 2006. MZmine: toolbox for processing and visualization of mass spectrometry based molecular profile data. Bioinformatics 22:634–636. https://doi.org/10.1093/bioinformatics/btk039.
58. Pluskal T, Castillo S, Villar-Briones A, Oresic M. 2010. MZmine 2: modular framework for processing, visualizing, and analyzing mass spectrometry-based molecular profile data. BMC Bioinformatics 11:395. https://doi.org/10.1186/1471-2105-11-395.
59. Pruesse E, Peplies J, Glockner FO. 2012. SINA: accurate high-throughput multiple sequence alignment of ribosomal RNA genes. Bioinformatics 28:1823–1829. https://doi.org/10.1093/bioinformatics/bts252.